

GEOPHYSICAL SURVEYS FOR DEFINING FAVORABLE STRUCTURES FOR URANIUM REMOBILIZATION IN WADI YOIDER, SOUTH EASTERN DESERT, EGYPT

I.M. Gaafar

Nuclear Materials Authority, Cairo, Egypt.
E-mail: ibrahim.gaafar@hotmail.com

المسوحات الجيوفيزيائية للتعرف على التراكيب الجيولوجية الهامة لإعادة انتقال اليورانيوم بوادي يودر، جنوب الصحراء الشرقية، مصر

الخلاصة: تهدف الدراسة الحالية الى تكامل البيانات الجيوفيزيائية للتعرف على التراكيب الجيولوجية الهامة لإعادة انتقال اليورانيوم بوادي يودر، جنوب الصحراء الشرقية، مصر. وقد تم عمل مسوحات حقلية تفصيلية باستخدام أجهزة المسح الإشعاعي الجامي الطيفي وأجهزة قياس شدة المجال المغناطيسي وأجهزة قياس الكهرومغناطيسي ذي التردد المنخفض. وقد عكس تفسير خرائط التوزيع الإشعاعي بمنطقة الدراسة بوضوح زيادة محتوى اليورانيوم وأن نسبة اليورانيوم إلى الثوريوم تتناسب طردياً مع قيم اليورانيوم وعكسياً مع قيم الثوريوم في نطاق القص الذي يمتد في الاتجاه شرق شمال شرق -غرب جنوب غرب مما يدل على إعادة تركيز اليورانيوم به حيث يصل تركيز اليورانيوم به الى ٧٥٠ جزء في المليون بينما يتميز نطاق القص الذي يمتد في اتجاه الشمال-الجنوب بمحتوى عالي من اليورانيوم يتراوح بين ١٠ إلى ١١٠ جزء في المليون. وتهتم هذه الدراسة بتتبع الشكل الهندسي المدفون لنطاق القص من خلال تفسير بيانات الشدة المغناطيسية والتوصيلية الكهربية. وتطبيق طريقة 3D-Euler deconvolution، تم تقدير أعماق التراكيب الجيولوجية والقواطع التي تتراوح من ٢٠ إلى ١٥٠ متر. وتمثل التراكيب الجيولوجية الممتدة في اتجاه شرق شمال شرق-غرب جنوب غرب، والتي يقع معظمها في الجزء الشرقي من منطقة الدراسة، الأعماق الضحلة والأقدم عمراً بينما تعتبر التراكيب الجيولوجية الممتدة في اتجاه شمال شمال غرب الأحدث عمراً والأكثر عمقاً والتي تصل إلى ١٥٠ متر وتتركز غالباً في الجزء الغربي من منطقة الدراسة. وقد أوضحت نتائج المسح الكهرومغناطيسي ذي التردد المنخفض باستخدام ترددين احدهما موازى لنطاق القص (١٧,٤ كيلو هرتز) والآخر عمودى عليه (١٧,١ كيلو هرتز) وأن نطاق القص يمتد في اتجاه شرق شمال شرق-غرب جنوب غرب الى حوالي ٦٠٠ متر ويتميز بتوصيل كهربى عالي مقارنة بصخور الجرانيت المحيطة وأنه يمتد في العمق ليصل إلى ٨٠ متر. ويعتبر ارتباط شادات اليورانيوم العالية مع التوصيل الكهربى الجيد بنطاق القص في منطقة الدراسة مؤشراً كافياً على وجود تمعدنات اليورانيوم وأنه يمثل بيئة جيدة لاحتواء وإعادة تركيز اليورانيوم المنقول.

ABSTRACT: Geophysical data integration was used for delineating the structural controlling U-remobilization in Wadi Yoider area, south eastern desert, Egypt. The area was studied using detailed ground gamma ray spectrometric, magnetic and VLF-EM surveys. The interpretation of the obtained ground gamma ray spectrometric maps clearly reflects the sharp increase of eU content. The eU/eTh ratios correlate positively with eU concentrations and negatively with eTh concentrations associated with the ENE-WSW trending shear zone indicating an increase in the U-potentiality than the surrounding granite. The N-S trending shear zone displays eU content ranging from 10 to 110 ppm. The ENE-trending shear zone is characterized by elongated uranium anomalies which values attaining up to 750 ppm. This study follows the expected subsurface geometry of the shear zone. 3-D Euler deconvolution method was applied to estimate source depths from the ground total magnetic-intensity data. The calculated source depths are in the range of 20 to 150 m. The shallow structures follow the ENE-WSW direction located mostly in the eastern part of the studied area. The major structures trending in the NNW-SSE direction have depths of up to 150 m and are associated mainly with its western part. The filtered VLF-EM maps of the two used frequencies (17.1 and 17.4 kHz) show an excellent agreement indicating that the shear zone is elongated in an ENE-WSW trend for about 600m in the E-W direction and distinguished with relatively high electrical conductivity. Most of the NW-SE trending faults suggest discontinuities in depth due to their left-lateral strike-slip displacements. The interpreted faults, with an ENE-WSW trend represent the main trend of the shear zone, through which hydrothermal solutions flowed causing high alteration and uranium mineralization.

INTRODUCTION

Wadi Yoider area is located very far in the south eastern desert of Egypt, between latitudes 22° 18' 23" N - 22° 19' 5" N and longitudes 36° 15' 52" E and 36° 16'

25" E at a distance of about 23 km to the southwest of Abu-Ramaad city (Fig. 1A).

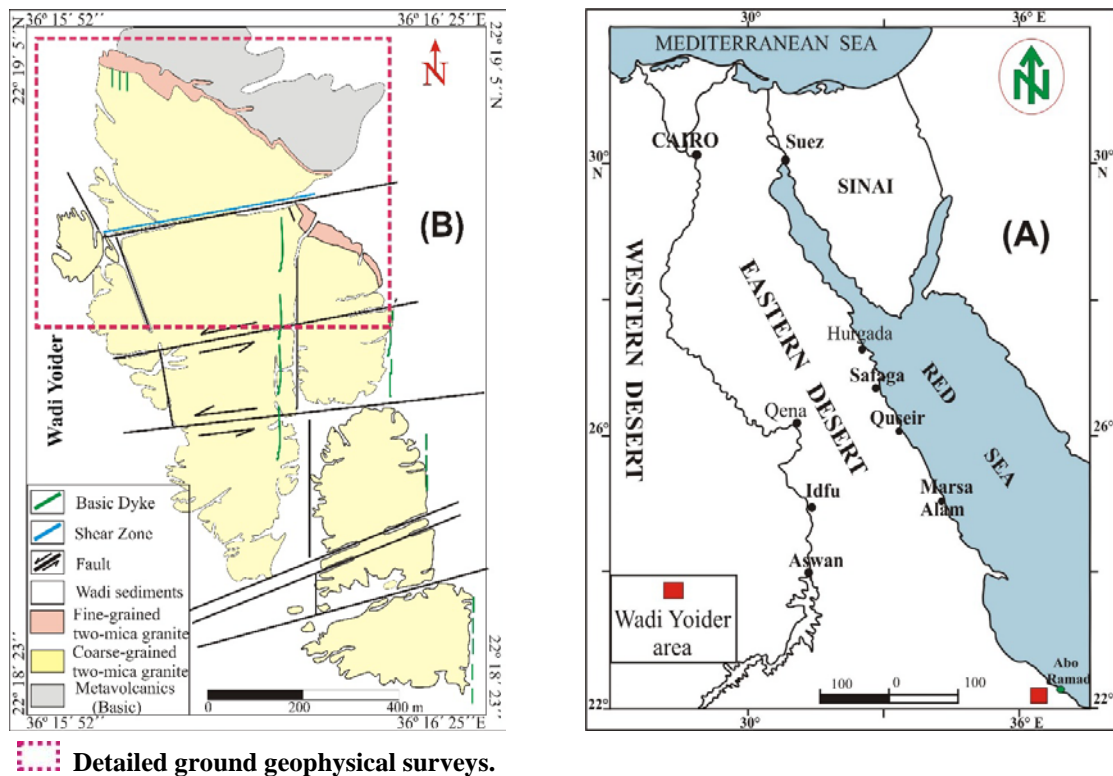


Fig. (1) A): Location map and B): Geologic map of Wadi Yoider area, south eastern desert, Egypt.

The advantage of the integration of some geophysical methods, such as electrical resistivity, electromagnetic and magnetic surveys as lithological and structural mapping tools was confirmed by many authors (e.g. Barker et al., 1992, Gaafar et al., 2010). Large areas of the world were covered by ground and airborne gamma-ray surveys and many national and regional radiometric maps were compiled and published (IAEA, 2003). Several occurrences of strongly-altered ultramafic units were located on the basis of correlation between aeromagnetic signatures and airborne radiometric results, and one of them directed to further exploration and located a mineralized zone (Airo, 2007). Radioactive minerals occur naturally in the geological environment associated with geological features like unconformity contact, veins, shear zones, and so forth (Bhaumik et al., 2004, Tuncer, et al., 2006). Such shallow subsurface structures can be best delineated by very low frequency electromagnetic method due to its advantage in detecting conducting structures. Uranium, being a metal, is highly conducting and, therefore, its presence in the subsurface rocks provides an excellent conductivity contrast between its deposit and the neighboring formations (Legault et al., 2008, Nimeck and Koch, 2008). During the last decades, VLF surveying was employed world-wide to identify conducting features in mineral exploration, geological, engineering and environmental problems (Oskooi and Pedersen, 2001; Smith et al., 2001; Becken and Pedersen, 2003).

In this study, it is intended through geological and magnetic mapping, to obtain the optimum conditions for

detecting the uranium-mineralization occurrence in a highly-magnetized shear zone in the study area. The exploration in Wadi Yoider area was directed to define the subsurface structural pattern for a vein type of uranium mineralization with a strong contrast in the properly of magnetic susceptibility.

VLF radio transmitters, operating in the 15–30 kHz frequency bandwidth, provide an electromagnetic source for geophysical investigation. The VLF method proved to be an effective exploration tool for massive sulphides, graphites, carbonaceous shales, sheared contacts, and fracture zones. Therefore, it was employed world-wide to identify conducting features in mineral exploration, geological, engineering and environmental problems (Chouteau et al., 1996; Gharibi and Pedersen, 1999; Oskooi and Pedersen, 2001; Becken and Pedersen, 2003). In this study, the strong contrasts in electrical conductivity provided direct exploration vectors for the uranium-mineralized materials through the use of VLF- EM technique.

GEOLOGY

The granite pluton which is located to the west of the investigated area was subjected to detailed studies comprising field geological and geophysical mapping by Gaafar (2005) and Gaafar et al., (2014). The ENE-WSW shear zone dykes dissecting the northern part of these granites are massive, fine-grained black groundmass, with alkali feldspar phenocrysts (Gaafar, 2005). Many promising criteria to locate uranium mineralization were reached, especially those related to the ENE-WSW shear zone (Gaafar et al., 2014; Gaafar,

2015). Many generations of silica as well as microgranite and shear zone dykes enriched in uranium were recorded (Ibrahim et al., 2009). Alteration processes superimposed the emplacement of these injections, are structurally-controlled and well defined through the ENE-WSW shear zone and the nearly perpendicular N-S fault set (Fig. 1B). This zone, which was the channels for the fluids, involved in all uranium concentrations, which may lead to the formation of a favourable U-mineralization in the study area.

The importance of the shear zone in remobilizing and concentrating uranium minerals make it useful to compile the expected subsurface extensions of this rock. According to the strong contrast between the magnetic susceptibilities of the shear zone, and the surrounding granites, magnetic survey was necessary for determining the expected subsurface extension of the shear zone and its contacts with the surrounding rocks. This is very important for determining and recommending the locations, dips and depths.

The detailed geological field work distinguished two main granitic phases in the studied area. The earlier one is the coarse-grained two-mica granite. The second latter one is the fine-grained two-mica granite, which is exposed in the northern part of the pluton as patches which crosscut the coarse-grained granite (Fig. 1B). The brecciated granite in this area is leucocratic and mainly composed of quartz, feldspars and muscovite/biotite mica. Some intensive alteration features, such as hematization and illitization are recorded, where a set of parallel N-S faults are present. This granite is highly weathered and its bulk volume disappeared and representing low land granitic masses. The process of uranium mobilization is very important as such altered rocks were subjected to mineralized-bearing solutions (Gaafar et al., 2014).

High magnetic intensity and high electrical conductivity anomalies as well as shallow subsurface signatures of uranium from three bore holes was recorded west Wadi Yoider area, in El-Sela Shear zone area (Gaafar et al., 2006 and Gaafar et al., 2014). The influence of the ENE-WSW and NNW-SSE structural trends in the successive structural events make its evolutionary history a suitable guide to describe the lithologic and structural history of Wadi Yoider area.

GROUND GAMMA-RAY SPECTROMETRIC SURVEY

Ground gamma ray spectrometric measurements were conducted to cover a variety of lithologies and various degrees of alterations associated with the uranium mineralization in the study area. The shear zone is characterized by abnormally high eU content (Gaafar et al., 2014, Gaafar et al., 2015). Several recent studies showed the usefulness of gamma-ray spectrometric surveys for abandoned mine site characterization (e.g. Winkelmann et al., 2001; Martin et al., 2006).

One field characteristic of the mineralized brecciated granite is its pervasive alteration and higher

degree of fractionation than normal fresh granite. The radon concentrations are aligned along the NNW direction, forming many anomalies with different amplitudes and different magnitudes ranging between 18000 and 190300 Bq.m⁻³ (Gaafar et al., 2010). This enrichment in uranium on the expense of both thorium and potassium is associated with the occurrence of discrete uranium minerals.

Field Procedure:

Ground radioelement concentration measurements were carried out over the studied area in the form of a uniform grid (40 m × 20 m). The measurements were conducted using a Czech-made Geophysica Brno GS-256 spectrometer, having a 0.35 L sodium iodide (NaI) thallium (TI) activated detector. The spectrometer is well calibrated on artificial concrete pads of NMA, containing known concentrations of K, U and Th. The radiation energy spectrum depicts the relative count rates in the range between 0.12 and 3.0 MeV. U, Th and K were determined by analyzing the gamma radiations from ²³⁸U, ²³²Th and ⁴⁰K, recorded at different windows (Chiozzi et al., 2000). For the determination of eU and eTh, the selected peaks and energy values were ²¹⁴Pb at 1.76 MeV and ²⁰⁸Tl at 2.62 MeV, respectively. Potassium was directly determined from the window centered at 1.46 MeV corresponding to the primary decay of ⁴⁰K.

Gamma-Ray Spectrometric Results:

Studies on the concentration and the distribution of the three naturally-occurring radioelements are of considerable interest in geophysics. They are useful in theoretical applications, such as modelling the underground thermal structure, because U, Th and K are the main sources of radiogenic heat in the rocks (Chiozzi et al., 2002). In the present study, the γ -ray spectrometric contour and ratio maps (K, eU, eTh and eU/eTh) for the study area were prepared and subjected to detailed interpretations.

Potassium (K %) map:

The potassium surface distribution contour map (Fig. 2) shows that the lowest potassium contour line values (<1.0 %) are associated mainly with Wadi sediments. The ENE-trending shear zone and the N-S trending one faults are well discriminated with their elongated shapes and low K levels. The two-mica granite shows potassium content, ranging from 2.1 to 5.3 %. It is encountered as zones of irregular shape that are mainly elongated in the two main structural trends in the study area (NNW-SSE and ENE-WSW). This increase in K content results from the highly-fractured, granite beside the intrusions of late-magmatic fine-grained granite.

Equivalent uranium (eU, ppm) map:

Both of the N-S and the ENE-trending shear zones are characterized by strong eU concentration anomalies (Fig. 3). The values, less than 2 ppm eU are observed over Wadi sediments around the granite. The eU range

(2-10 ppm) is shown over the coarse-grained two-mica granite. It is encountered as zones with different shapes, sometimes controlled by the main fault trends in the study area.

The N-S shear zone displays sharp gradients of eU-content ranging from 20 to 140 ppm. Such high range or level is encountered as elongated domains trending in the NNW-direction along the main faults. These eU anomalies reflect secondary uranium remobilization along these fault zones.

The ENE- trending shear zone, which crosses the northern part of coarse-grained two-mica granite, plays an essential role in uranium remobilization processes. It is characterized by elongated anomalies trending in the E-W direction, with values >90 ppm eU. These altered rocks were subjected to mineralization-bearing solutions, where the shear zone acts as a good trap for U-rich fluids.

Equivalent uranium content of the brecciated granite along the ENE-WSW shear zone attains values up to 700 ppm, with relatively low eTh and K contents. Such locations proved to possess high U-potentialities in the study area. This high U-potentiality is typically associated with the alteration of the sheared rocks, which are associated with uranium mineralization.

Equivalent thorium (eTh, ppm) map:

Thorium content usually reflects the original rock varieties and the fractionation in this type of granites, when thorium content increases. Therefore, eTh content image map (Fig. 4) shows marked discrimination between the two-mica granite and the Wadi sediments and metavolcanics. The two-mica granites have moderate values of eTh ranging from 6 to 28 ppm. The eTh along Wadi sediments have values ranging from less than 0.2 to 5 ppm. They define zones with different shapes, distributed all over the whole Wadi sediments. The unaltered shear zone occurring in the northern part of the two-mica granite possesses elongated low values.

eU/eTh ratio map:

The general view of the surface eU/eTh ratio distribution map of the study area (Fig. 5) indicates that the ENE-WSW shear zone shows promising anomalies elongated in the E-W direction in the northern part of the study area. These strong anomalies show raised amplitudes, resulting in obvious exploration targets. Meanwhile, the N-S shear zone shows also high content of eU over eTh levels, trending in the NNW-direction. A fractured controlled U-mineralization is located within the shear zone in the granite. This vein type mineralization possesses higher U-content many times greater than the granite, leading to an increase in the U-potentiality, which might lead to U-mobilization and possibly local uranium entrapment in the study area.

GROUND MAGNETIC SURVEY

Magnetic method, being a faster economical and versatile geophysical tool, may help reveal both large and small-scale features, including differences in basement rock types, magmatic intrusions, basement surface and fault structures (Vasanthi et al., 2006). The

concentration of magnetic minerals or their excessive destruction by hydrothermal alterations, especially along tectonic structures enhances the use of this method for the detection of geological structures (Plumlee et al., 1992).

Field Procedure:

The present ground magnetic survey includes only the northern part of the studied area that is crossed by the ENE-trending shear zone attaining 640 m in length and 740 m width of (Fig. 6), using a uniform square grid of (40×40 m). All the ground magnetic measurements were collected using the Scintrex proton precession magnetometer and the VLF-EM; Canada-model ENVI.

Magnetic Results and Interpretation

The exploration in the study area was directed to define the subsurface structural pattern for the uranium mineralization, with contrasts in magnetic susceptibility. Besides, the deep penetration of the magnetic data provides direct exploration vectors for determining the appropriate drilling locations for the expected subsurface uranium mineralization.

The total magnetic intensity map (Fig. 6) shows strong positive magnetic anomalies, directly over the basic metavolcanics, probably caused by deep sources. The sharp contacts between the outcropping granites and basic metavolcanics at the northern parts of the geologic map are obvious on various magnetic maps. They also confirm good agreement of the magnetic intensity data with surface geological structures, which indicate of the two-mica granite thrust over the basic metavolcanics that have huge extensions in depth. The total magnetic field intensity map (Fig. 6) contains many nearly-circular positive anomalies located to the north (having an amplitude of about 230 nT) and extend over Wadi sediments to width about 250 m, with small surficial outcrops of basic metavolcanics. This indicates continuity of the basic metavolcanics in the subsurface, which is responsible of these magnetic anomalies. The negative counterpart of this broad magnetic anomaly is about 50 nT. The shear zone is located along the contact between the high and low magnetic intensity field that is elongated in the E-W direction, and extends to about 700m. It is characterized by high eU content, reaching more than 700 ppm. This indicates that the uranium enrichment is post-magmatic due to the remobilization of uranium from the adjacent granite into the shear zone. Comparing the magnetic contour map with its geologic background (Fig. 6), it is evident that the magnetic anomalies possess broad limits in depth than the exposed basic metavolcanics.

Generally, the total magnetic intensity values decrease towards the southern part of the studied area, i.e., from 40350 nT to 40318 nT (Fig. 6). This difference is due to the response of two-mica granites, which have broad extensions underneath Wadi sediments. The prominence of sudden changes in the spacing of the magnetic contours, which trend mostly in the NNW-direction, suggests discontinuities in depth, possibly subsurface major faults. These faults caused displacements for the E-W trending anomalies.

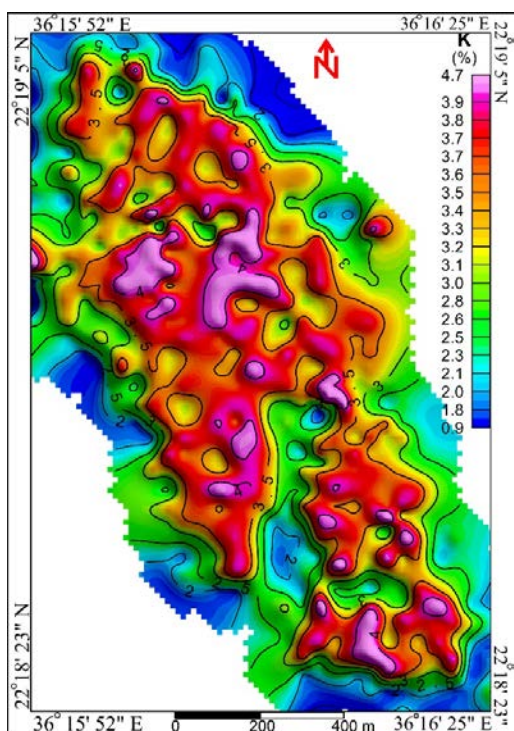


Fig. (2): Potassium (K, %) image and contour map of Wadi Yoider, south eastern desert, Egypt.

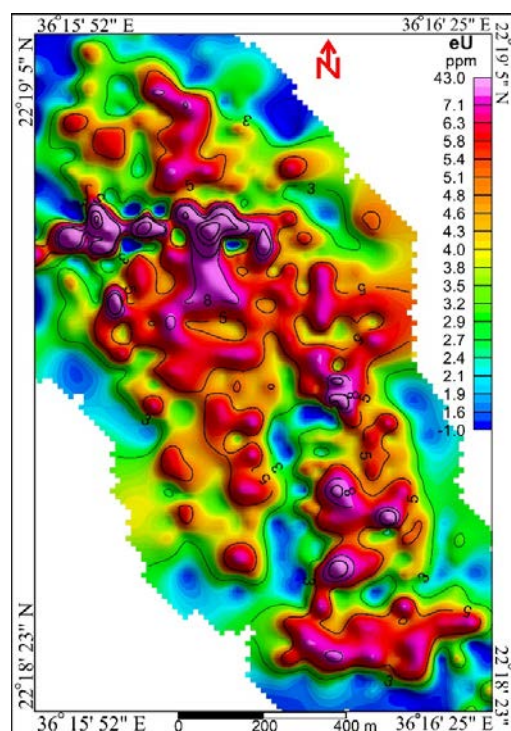


Fig. (3): eU (ppm) image and contour map of Wadi Yoider area, Southern E D, Egypt.

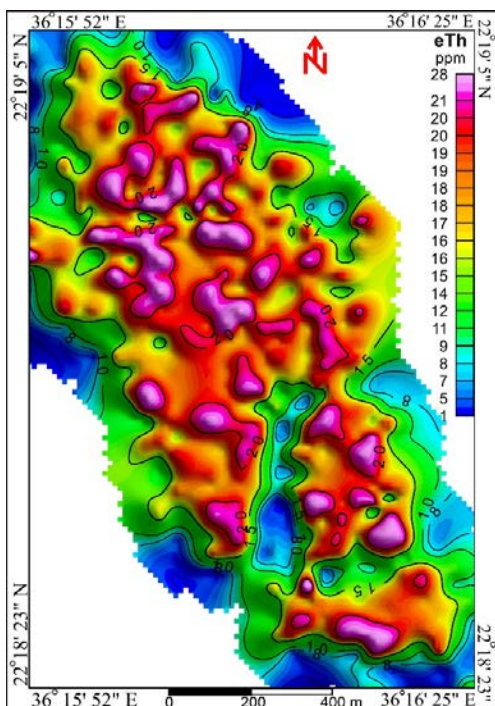


Fig. (4) : eTh (ppm) image and contour map of Wadi Yoider area, south eastern desert, Egypt.

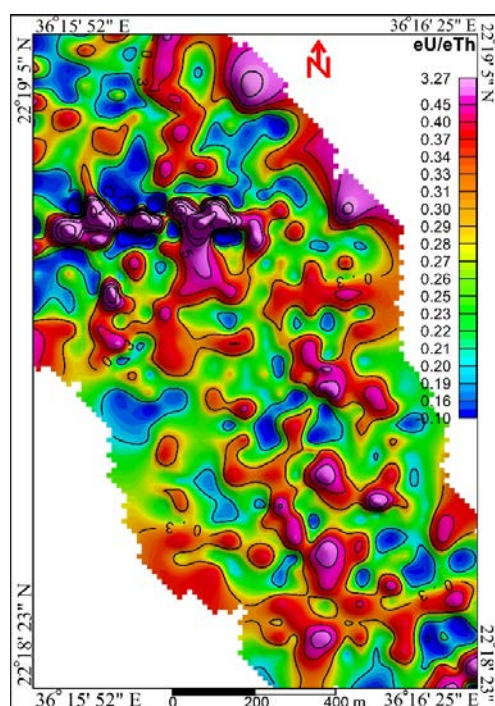


Fig. (5) : eU/eTh ratio image and contour map of Wadi Yoider area, Southern E D, Egypt.

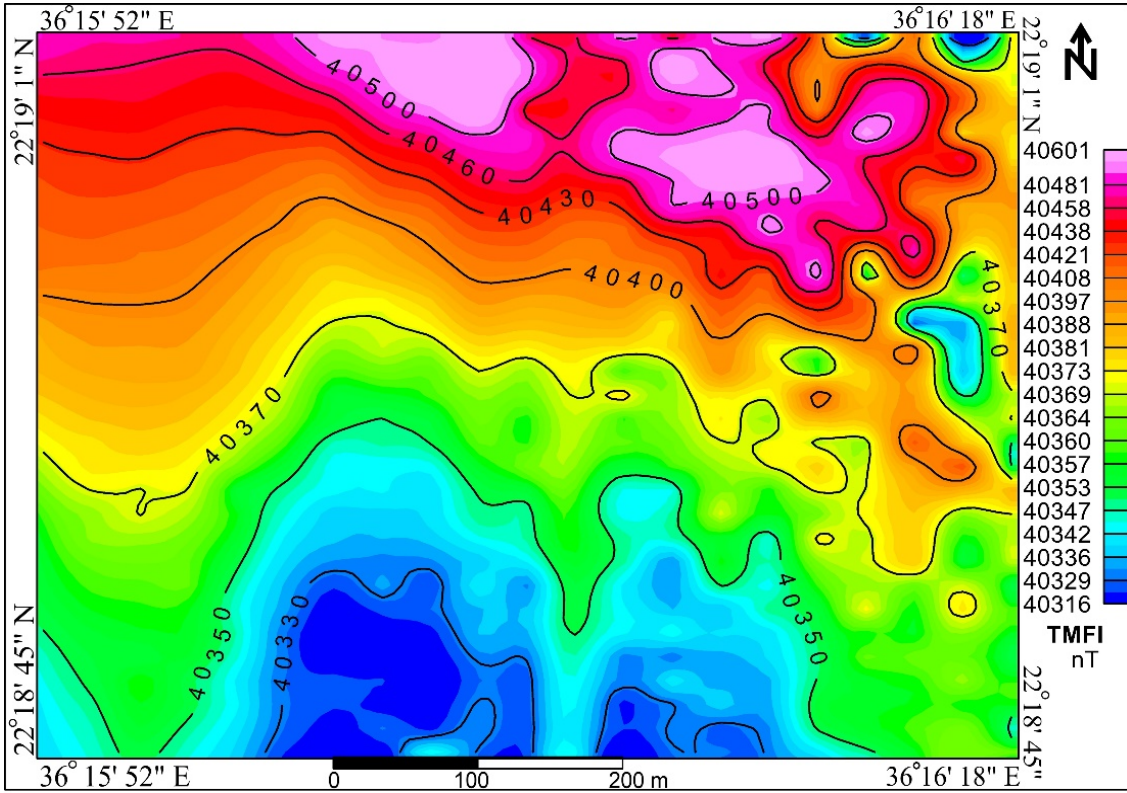


Fig. (6): Total magnetic field intensity (TMFI in nT) image and contour map for Wadi Yoider area, south eastern desert, Egypt.

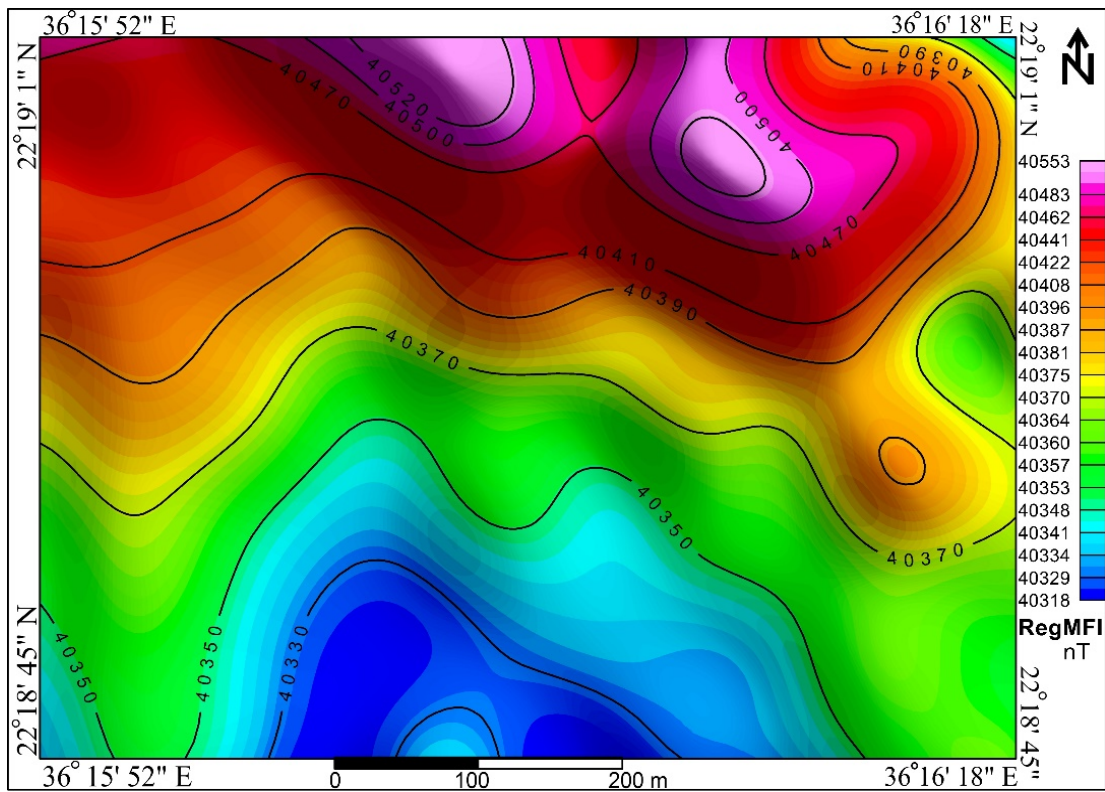


Fig. (7): Regional magnetic field intensity (Reg MFI in nT) image and contour map for Wadi Yoider area, south eastern desert, Egypt.

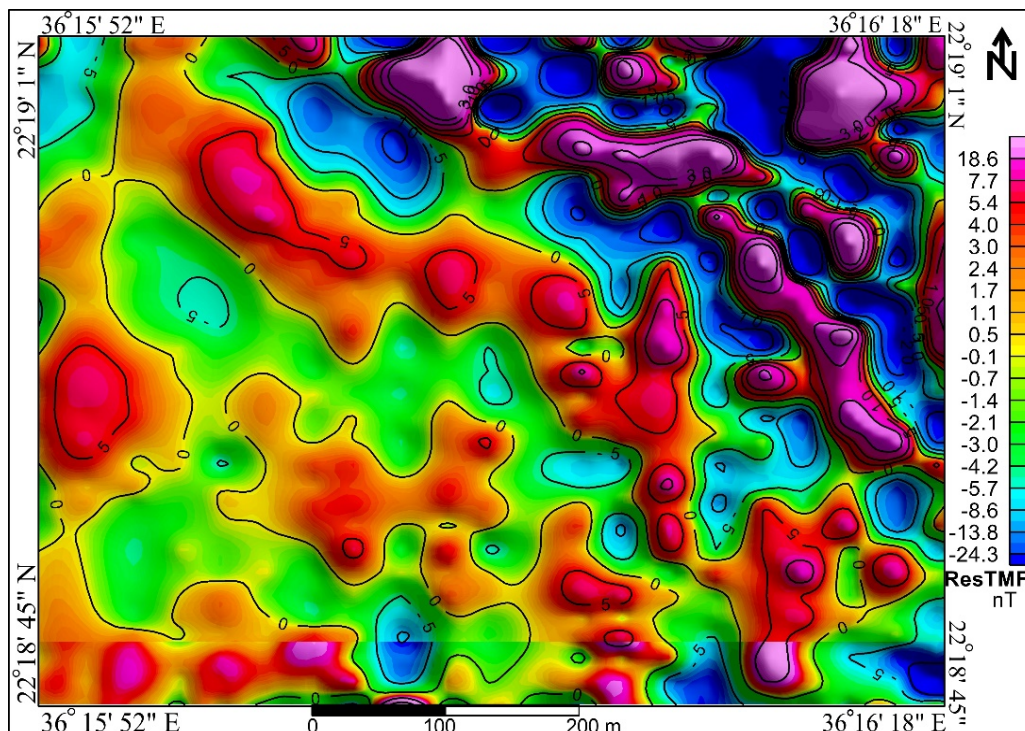


Fig. (8): Residual magnetic field intensity (Res MFI in nT) image and contour map for Wadi Yoider area, south eastern desert, Egypt.

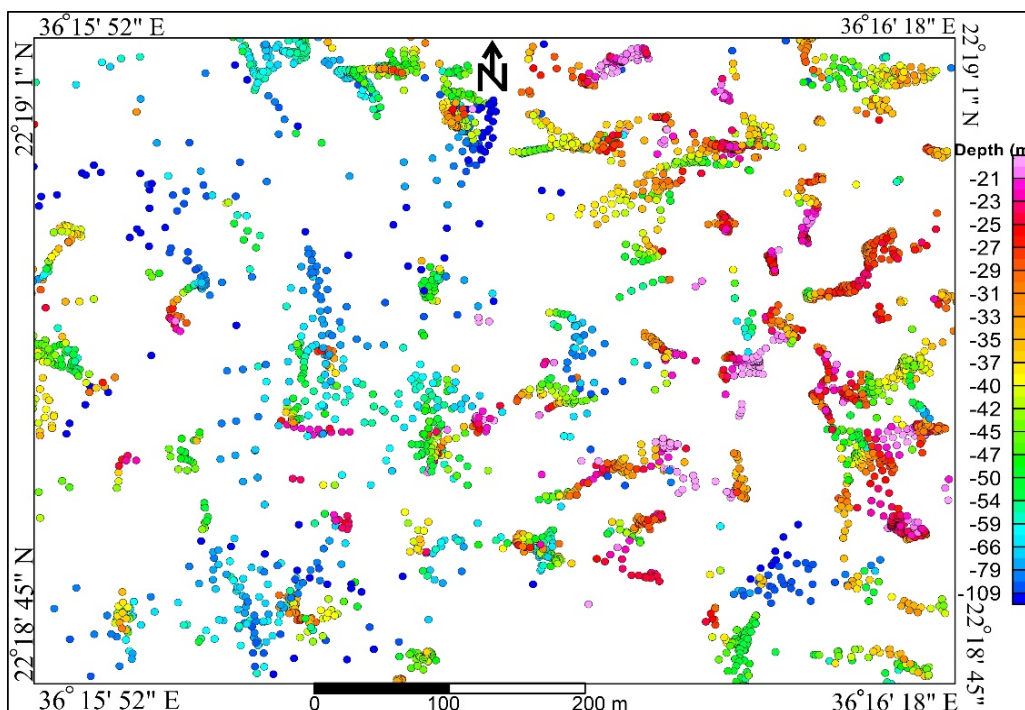


Fig. (9): Euler Deconvolution (SI=1, Dyke) map of reduced to the pole (RTP) magnetic map for Wadi Yoider area, south eastern desert, Egypt.

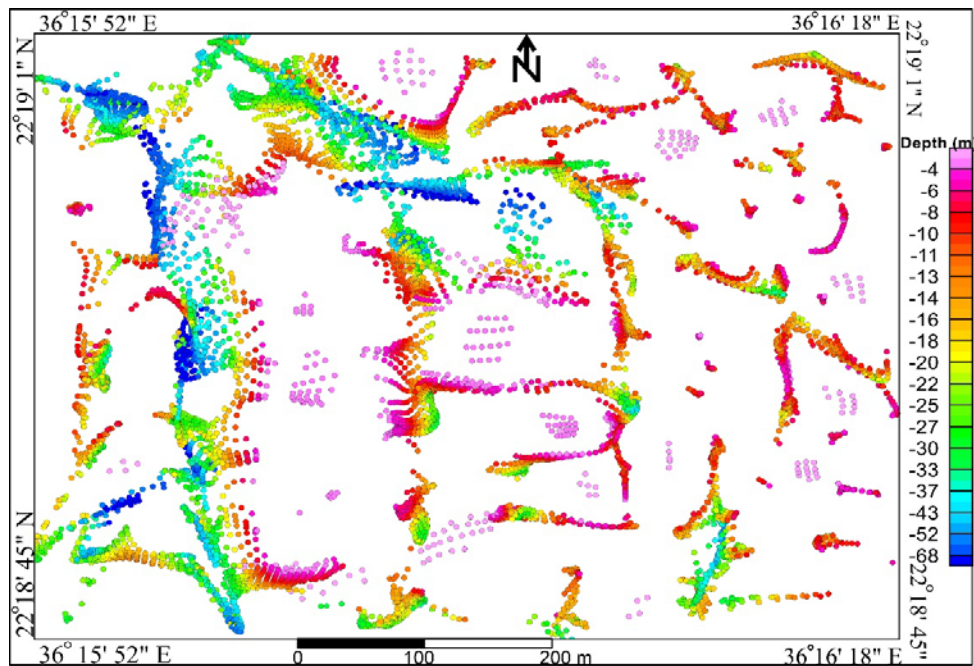


Fig. (10): Euler Deconvolution (SI=0, Contact) map of RTP magnetic map for Wadi Yoider area, south eastern desert, Egypt.

The Butterworth method has been used for magnetic regional-residual separation. The regional magnetic component map (Fig. 7) shows strong positive magnetic anomalies located at the northern parts of the study area, coinciding with metavolcanics and Wadi sediments. These anomalies are due to buried basic rocks, over which the granites are thrusts. The low magnetic anomaly (Fig. 7) is associated with the granitic body becomes broader than on the total magnetic field intensity map (Fig. 6). This is due to the deep causative source.

The residual magnetic map (Fig. 8) shows narrow magnetic anomalies that are elongated in the WNW-ESE direction in the northeastern part of the study area. The absence of any magnetic expression in the northwestern part of the study area may be explained by the non-existence of magnetic source bodies near the surface. The linearity and continuity of numerous anomalies of N-S trend suggest the presence of a parallel system which dissected the two-mica granites (Fig. 8).

Depth Estimation:

The objective of the 3D Euler deconvolution process is to determine the shapes and corresponding depth estimates of geologic sources of the magnetic anomalies. Depth estimation by Euler deconvolution technique was used for delineating cluster depth maps of dyke structural index (Fig. 9) and contact structural index (Fig. 10). This technique provides automatic estimates of source location and depth.

Euler deconvolution is both a boundary finder and depth estimation method. It is commonly employed in magnetic interpretation, because it requires only a little

prior knowledge about the magnetic source geometry, and more importantly, requires no information about the magnetization vector (Thompson, 1982; Reid et al., 1990). The most critical parameter in the Euler deconvolution is the structural index, N (Thompson, 1982). Therefore, by changing N , the geometry and depth of the magnetic sources can be estimated. For magnetic data, physically plausible N values range from 0 to 3.

Several structural index values were assigned for structural index ($N = 0$, $N = 1.0$, $N = 2.0$) of the extensions of linear clustering of Euler solutions gave colored points similar to the main trends of the two previous methods. In addition, the Euler solution map reveals new deep contacts, which represent accurate-style trends in the southeastern part of the study area. The Euler plot (Fig. 9) clearly defines the solution for depths that range from 5 m to 100 m. Most of the Euler solutions in the eastern part of the study area show rather shallow depths of about 40 m for the possible causative sources. The depths in the western part of the study area are situated at deeper depths of about 30 to 120 m. In the northwestern part of the study area, Euler plots show non-uniform depth distribution from shallow to deeper depths. The solution clusters are controlled with the main structural trends of the studied area that are elongated in the N-S, E-W and NNW directions.

Structural Interpretation:

The analysis and geological interpretation of the magnetic trends in the study area reveal that the main structural trends is represented by the NNW-SSE direction as well as the ENE-WSW direction (Figs. 11, 12).

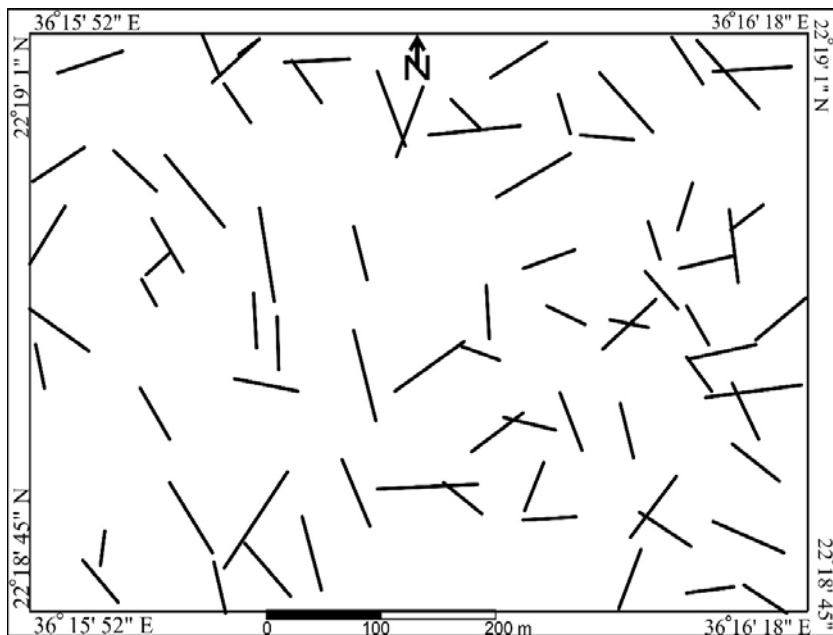
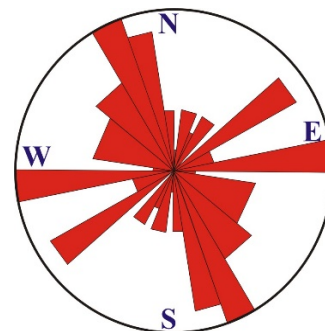
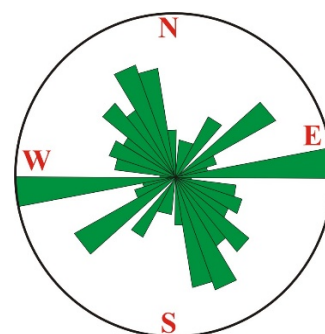


Fig. (11) Interpreted lineaments of dykes with their rose diagram as deduced from Euler map for Wadi Yoider area, Southern E D, Egypt.



Number



Length

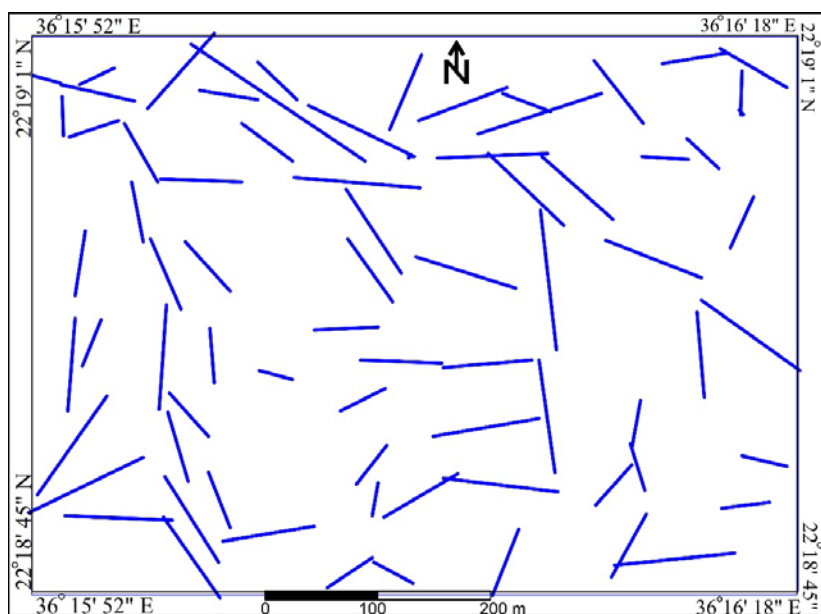
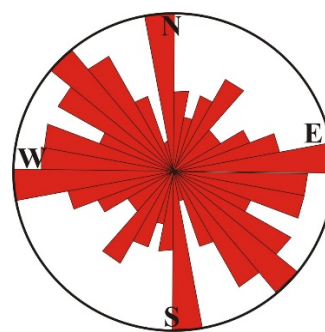
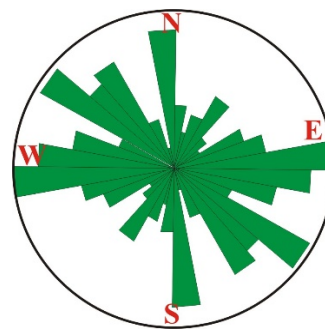


Fig. (12) Interpreted lineaments of contacts fractures with their rose diagram as deduced from Euler map for Wadi Yoider area, Southern E D, Egypt.



Number



Length

The NNW-SSE direction represents the latest trend, which affected all the rocks of the study area. Meanwhile the ENE-WSW direction is considered the older one, mostly attributed to a northern shear zone. The ENE-trending shear zone is intersected by a NNW-trending left-lateral strike-slip fault system, as shown on the interpreted structural lineament map (Figs. 9, 10) and as deduced from the dyke and contact data maps (Fig. 12).

The ENE-trending lineaments, i.e., the interpreted group of faults, represents the main trend of the shear zone, through which hydrothermal solutions were flowing, causing high alteration and uranium mineralization.

This trend denotes an important structural phase that controls another set of microgranite, quartz, kaolinitization and brecciated granite dykes in the study area. These dykes are highly radioactive and some of them are associated with uranium mineralization. Therefore, it is worthy to mention that the complicated lithologic and structural history of the study area represent a promising criteria for uranium fertility. Another major fault or shear zone, trending parallel to the main shear zone, mainly lies at the northern part of the studied area. This fault or shear zone is of a deep-source. It is dissected and displaced by the NNW-trending faults.

VERY LOW FREQUENCY (VLF) SURVEY

Because of the easy operation of the instrument, high speed of field survey, and low operational cost, this method was found to be very suitable for rapid preliminary surveys, besides its wide use in many geophysical studies, since 1960 (Bernard and Valla, 1991; Benson et al., 1997; Sharma and Baranwal, 2005). The VLF represents a valuable help to geological mapping. This method is a reconnaissance electromagnetic geophysical tool for mapping near-surface structures (Oskooi, 2004) using relatively simple instruments. It was used successfully to investigate faults all over the world; examples include Nojima fault and Ogura fault (Yamaguchi et al., 2001), non-mineralized shallow fault zones (Jeng et al., 2004), groundwater-bearing zones (Sharma and Baranwal, 2005).

VLF Field Procedure:

The utilized instrument was the Scintrex VLF (ENVI VLF), Toronto, Canada, using two orthogonal VLF transmitters of frequencies $F_1=17.1$ kHz, and $F_2=17.4$ kHz. For tilt angle measurements, magnetic field coupling with the fracture zone is important. The mid-frequencies ($F=17.4$ kHz) were parallel to the E-W trend of the sheared shear zone, whereas the low frequency ($F=17.1$ kHz) is perpendicular to it.

Results and Interpretation of VLF-EM Survey:

The two used frequencies (17.1 and 17.4 kHz) displayed a remarkable agreement, in locating the shear zone conductors (Figs. 13 and 14). The granitic rocks are associated with relatively weak conductivity zones that generally follow the NW- and E-W trending lineaments. Meanwhile, the shear zone is located in the

central parts of the study area, within a strong conductive zone that is elongated in the ENE-WSW direction (Figs. 11 & 12).

Discussion of the results of Geophysical Profiles and VLF-EM Pseudo-Sections

The combination of geophysical models represents a valuable tool for increasing the understanding of subsurface geometries. Better subsurface models add value to mineral exploration projects. The regular distribution of geophysical data allows lithologies and structures to be continued into areas not exposed on the surface. VLF pseudo-sections are fast and accurate in depicting the subsurface structures. They are widely used for VLF data interpretation. This imaging technique was used to produce apparent current density cross-sections in the present study. Four profiles, namely, L1, L2, L3 up to L4, covering the whole studied shear zone, with intervals of 120m and profile lengths ranging from 500m to 550m were studied (Fig. 15). For the interpretation of the subsurface geometry, apparent current density cross-sections with depths were conducted using the acquired VLF data along all the profiles using Karous-Hjelt filter (1983). These apparent current density cross-sections are presented on four Figures (15–18), below the real and imaginary anomaly plots obtained from the VLF data acquired in the field. Results for surface gamma ray spectrometric measurements of eU, eU/eTh and eU/K are also shown as line plots along with VLF anomalies for every individual profile (Figs. 16–17). The shear zone is characterized by strong variation in the electrical conductivity. This is typically due to the alteration of the sheared rocks to mineralized clays causing an increase in their conductivities, whereas the adjacent granites show low conductivities (Figs. 13, 14, 15). This is best developed along the central parts of the study area, where shearing and alteration show significantly high conductivity values.

Profile (L1) lies 160 m from the west of the studied area (Fig. 16). Here, the VLF anomaly curves indicate two main conductive features, one being shallow and another is deep. The apparent current density cross-section shows the presence of one low conducting and another high conducting structures between stations 50 m and 70 m and 120 m and 240 m, respectively (Fig. 16). The later conductor is more conductive and wider than the other one. Uranium content is observed to be high above this conductor, with a peak value of 60 ppm at the station 160 m. The eU/eTh and eU/K ratios reach 3 and 16 respectively. The magnetic intensity is very low in the southern part of this profile (L1) and increases gradually towards the north, due to the buried metavolcanics.

Profile (L2) lies 120 m east of the profile (L1) (Fig. 17). The VLF anomaly curves show two main conductive features. The apparent current density cross-section indicates the presence of conducting zones between stations 200m and 320m as well as 350m and 450m. The strong conductor of high anomaly is steeply dipping to the north. It is also well discriminated by its association with high uranium anomaly.

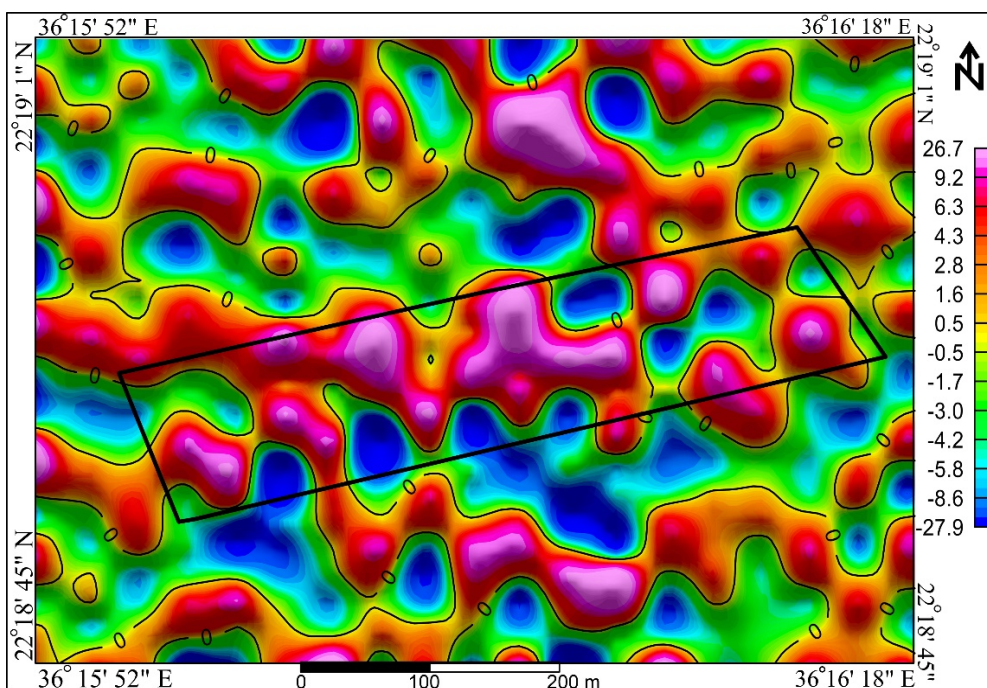



Fig. (13): VLF-EM Fraser filtered data (F=17.1 kHz) image and contour map for Wadi Yoider area, south eastern desert, Egypt.  Shear zone

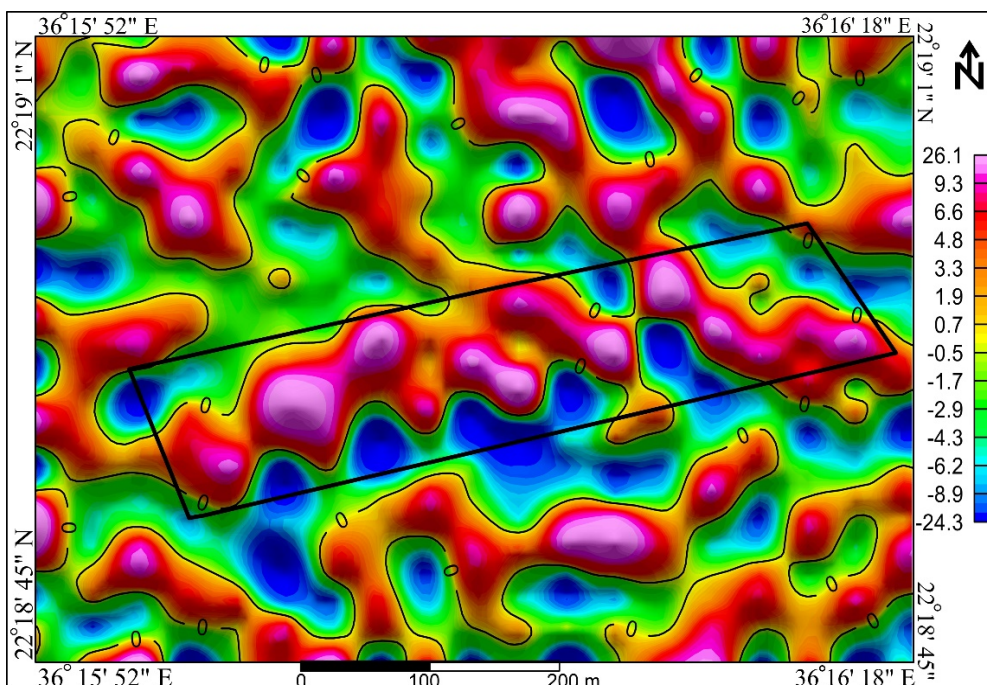



Fig. (14): VLF-EM Fraser filtered data (F=17.4 kHz) image and contour map for Wadi Yoider area, south eastern desert, Egypt.  Shear zone

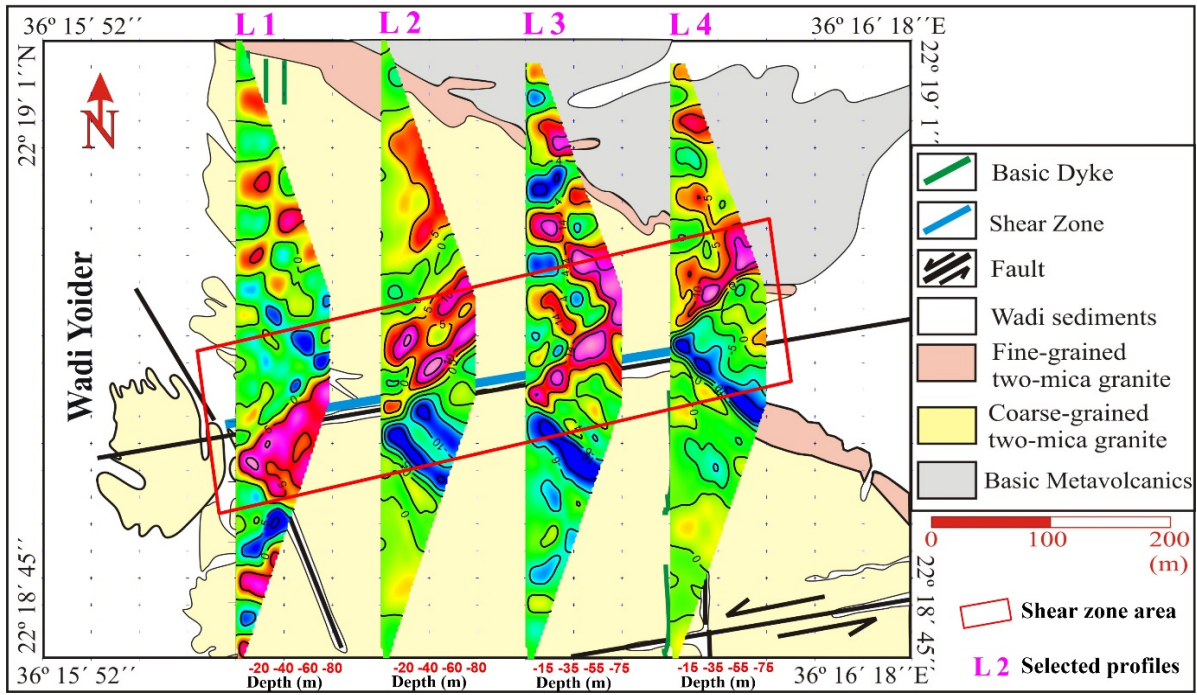


Fig. (15): VLF pseudo-sections superimposed on the geology map of Wadi Yoider area.

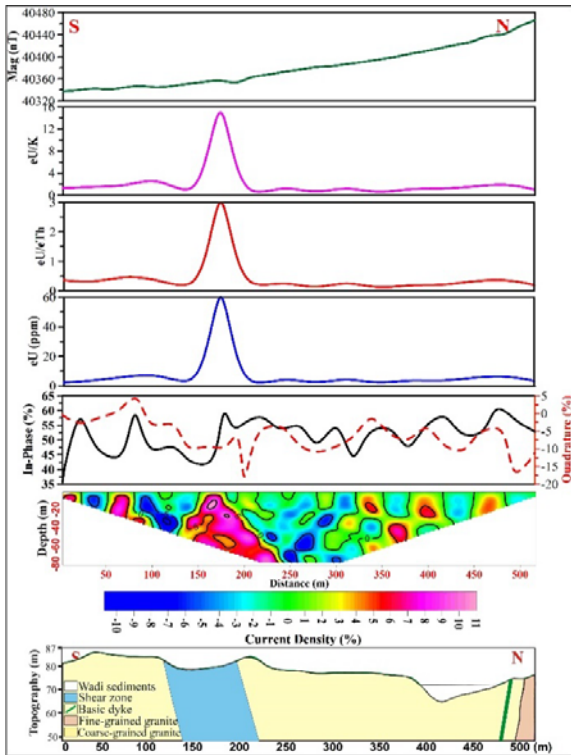


Fig. (16): L1, VLF pseudo sections, eU, eU/eTh, eU/K profiles and interpreted models for Wadi Yoider area.

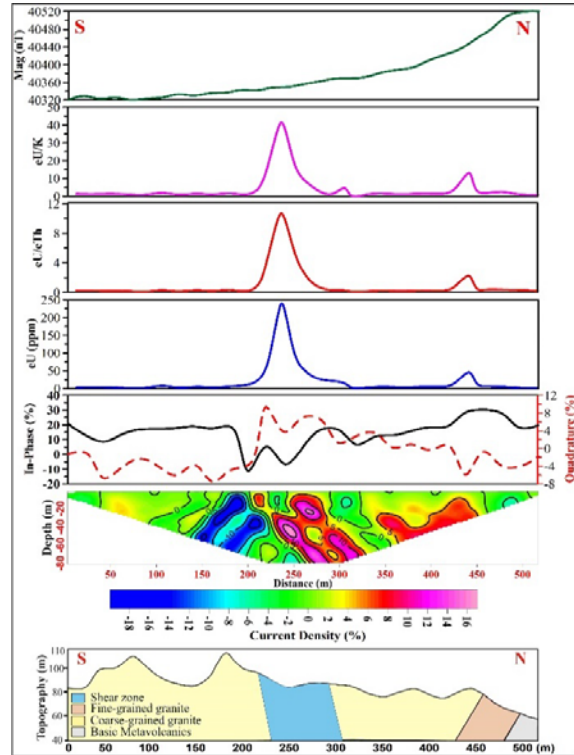


Fig. (17): L2, VLF pseudo-sections, eU, eU/eTh, eU/K profiles and interpreted models for Wadi Yoider area.

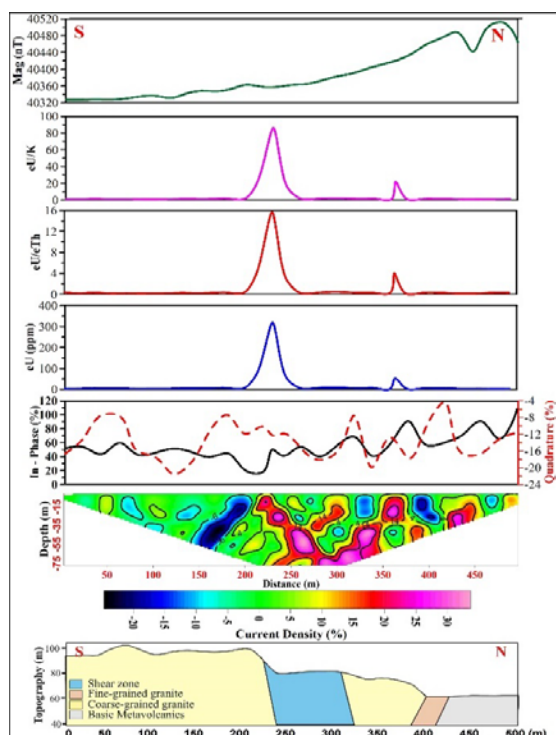


Fig. (18): L3, VLF pseudo-sections, eU, eU/eTh, eU/K profiles and interpreted models for Wadi Yoider area.

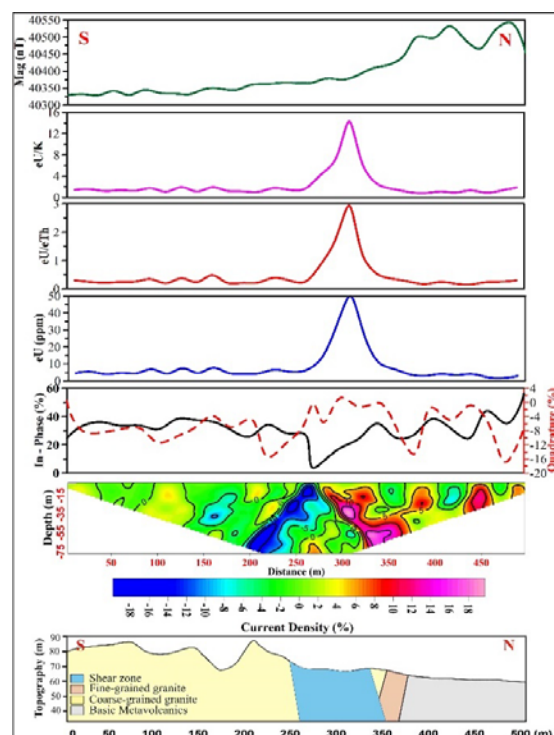


Fig. (19): L4, VLF pseudo-sections, eU, eU/eTh, eU/K profiles and interpreted models for Wadi Yoider area.

The values of its eU, eU/eTh and eU/K reach 250 ppm, 12 and 50 respectively, and are located at the station 250m (Fig. 17). On the other hand, the northern anomaly shows the moderate contents of eU, eU/eTh and eU/K that attain 45 ppm, 2.3 and 13 respectively. The magnetic intensity increases gradually from south to the north due to the presence of basic metavolcanics.

Profile (L3) is located at the center of the study area 120 m away from the profile no. (2) (Fig. 17). Both input and quadrature VLF curves indicate the existence of two conductive features around stations 220m and 370 m (Fig. 18). Another big conductive body, with a width of about 30 m, near the surface that increases gradually with depth reaching about 70 m at depth 80 m.

The current density of this big body reaches to about 34 % indicating a highly conductive source as shown on the apparent current density cross-section (Fig. 18). The radiometric data show high anomalous radioactivity in the center of the profile, with anomalies of eU, eU/eTh and eU/K whose values reaching to 320 ppm, 16 and 82 respectively, and are found above the station 220 m (Fig. 18).

Profile (L4) lies 120 m east of profile (L3) as shown in figures (15, 19). VLF anomaly curves indicate the presence of two conductors. Current density section traces the two conductive features between stations 270m and 380m and 430 m and 460 m (Fig. 19). The southern one is the highest conductive anomaly that

associated with the shear zone, compared to the northern one. The VLF-EM curves show marked changes in polarity along the shear zone. This reveals an anomaly around the same location, with the shapes and consistent with a conductive target. The uranium curves indicate that the conductivity is essentially due to the shear zone mineralization, with no contribution from the adjacent granite. There is one peak region of uranium and their ratios around station 300m (Fig. 19). This wide VLF-EM anomalies typical of a good conductor, which is in agreement with the eU, eU/eTh and eU/K values 50 ppm, 3.0, 14.

CONCLUSION

The eU and eU/eTh ratio distribution map indicate that the two-mica granite shows promising anomalies. Their spectrometric signatures are characterized by high anomalies that are elongated in the N-S direction, in the southeastern part of the study area. These vein type mineralization process possesses higher U-content many times greater than the granite, leading to an increase in the U-potentiality, which might lead to U-mobilization and possibly local uranium entrapment.

According to the strong contrast between the magnetic susceptibilities of the metavolcanics and the surrounding granites, magnetic survey succeeded in determining the expected subsurface extension of the shear zone at the unconformity contact. The interpreted magnetic structural map, for the study area, is dissected

by many structural lineaments, which have different directions indicating a complex tectonic history and several events of deformation. Most of the NNW-trending faults cause left-lateral strike-slip displacements and are associated with U-enrichment. The ENE-structural trending faults, interpreted as the oldest group of faults, represent the main trend of the shear zone, through which hydrothermal solutions flowed, causing the high alterations and uranium mineralization.

The coincidence of anomalous high radioactivity with the conductive zones and their correlation with radioactive bands observed in Wadi Yoider area confirms the presence of uranium mineralization. This can represent a sufficient indication to that target as uranium vein-type and a good trap for uranium-rich fluids or probably a uranium deposit. The obtained models by the pseudo-sections of the VLF-EM data strongly suggest that the volume of the shear zone at the study area increases with depth that continued for more than 78 m.

Accordingly, it would be promising for drilling operations to evaluate the expected Wadi Yoider vein type uranium mineralization.

REFERENCES

- Airo, M.L., 2007.** Application of aerogeophysical data for gold exploration: implications for Central Lapland Greenstone Belt. In: Juhani Ojala, V. (Ed.), *Gold in the Central Lapland Greenstone Belt, Finland*, Geological Survey of Finland, V. 44, pp. 171–192.
- Barker, R.D., White, C.C. and Houston, J.F.T., 1992.** Borehole siting in an African accelerated drought relief project. In: Wright, E. P., Simon, S. (Eds.), *Hydrogeology of Crystalline Basement Aquifers in Africa*, Geological Society V. 66, pp. 183–201.
- Becken, M. and Pedersen, L.B., 2003.** Transformation of VLF anomaly maps into apparent resistivity and phase. *Geophysics* V. 68, pp. 497–505.
- Benson, A.K., Payne, K.L. and Stubben, M.A., 1997.** Mapping groundwater contamination using DC resistivity and VLF geophysical method — a case study. *Geophysics*, V. 62, pp. 80–86
- Bernard, J. and Valla, P., 1991.** Groundwater exploration in fissured media with electrical and VLF methods. *Geoexploration*, V. 27, pp. 81–91.
- Bhaumik, K., Bhattacharya, T., Acharyulu, A., Srinivas, D. and Sandilya, M.K., 2004.** Principles of radiometry in radioactive metal exploration, Physics Lab, AMD Complex, Jamshedpur, India.
- Chiozzi, P., Pasquale V. and Verdoya, M., 2002.** Heat from radioactive elements in young volcanics by gamma ray spectrometry. *J. Volcanol. Geotherm. Res.*, V. 119, pp. 205–214.
- Chiozzi, P., Pasquale, V., Verdoya, M. and De Felice, P., 2000.** Practical applicability of field gamma ray scintillation spectrometry in geophysical surveys. *Appl. Radiat. Isotopes* V. 53, pp. 215–220.
- Chouteau, M., Zhang, P. and Chapellier, D., 1996.** Computation of apparent resistivity profiles from VLF-EM data using linear filtering. *Geophys. Prospect.*, V. 44, pp. 215–232.
- Fraser, D.C., 1969.** Contouring of VLF-EM data: *Geophysics*, V. 34, pp. 958–967.
- Gaafar, I.M., 2005.** Applications of geological and geophysical survey for defining the uranium potentiality of some younger granites in the Eastern Desert of Egypt. Ph. D. Thesis Fac. of Sc., Mansoura Univ., Mansoura, Egypt, 180 p.
- Gaafar, I.M., Hosni H.G., Ibrahim T. M. and Ammar S. E., 2006.** Gamma-ray spectrometry studies for a promising vein type uranium mineralization, south eastern desert, Egypt. 4th International Symposium on Geophysics, Tanta, pp. 445–456.
- Gaafar I.M., Nigm, A.A. Ibrahim T.M. and Hosny A.A., 2010.** Geophysical signature of the uranium mineralized quartz veins of Wadi Eikwan, south eastern desert, Egypt. *Egyptian Geophysical Society, EGS Journal*, V. 8, No. 1, pp. 181–190.
- Gaafar I.M., Cuney M. and Gawad, A., 2014.** Mineral chemistry of two-mica granite rare metals: impact of geophysics on the distribution of uranium mineralization at El-Sela shear zone, Egypt. *Open Journal of Geology*, V. 4, pp. 137–160.
- Gaafar I.M. 2015.** Application of gamma ray spectrometric measurements with VLF-EM data for tracing buried vein type uranium mineralization, South eastern Desert, Egypt. (In Press)
- Gaafar I.M., Aboelkheir H. and Baiumi, M.B., 2015.** Integration of gamma-ray spectrometric and aster data for uranium exploration in Qash Amer El-Sela area, Southeastern Desert, Egypt. (In Press)
- Geosoft Inc., 1995.** Geosoft mapping and processing system. Geosoft Inc., Toronto, Canada.
- Gharibi, M. and Pedersen, L.B., 1999.** Transformation of VLF data into apparent resistivities and phases. *Geophysics*, V. 64, pp. 1393–1402.
- IAEA, 2003.** Guidelines for radioelement mapping using gamma-ray spectrometry data. IAEA-TECDOC-1363, Vienna, 173p.
- Ibrahim, T.M., Abd-Elghany M.S., Ali, K.G. and Gaafar, I.M., 2009.** Characterization of new surficial uranium deposit in El-Sela area, south eastern desert, Egypt. *Annals Geol. Surv. Egypt*, V. 31, pp. 405–415.
- Jeng, Y., Lin, M.J. and Chen, C.S., 2004.** A very low frequency-electromagnetic study of the geo-environmental hazardous areas in Taiwan. *Environmental Geology*, V. 46, PP. 784–795.
- Karous M. and Hjelt S.E., 1983.** Linear filtering of VLF dip-angle measurements. *Geophysical Prospecting*, V. 31, No. 5, pp. 782–794.

- Legault J.M., Carriere D. and Petrie L., 2008.** Synthetic model testing and distributed acquisition DC resistivity results over an unconformity uranium target from the Athabasca Basin, northern Saskatchewan, Canada. *The Leading Edge*, V. 27, No. 1, pp. 46–51.
- Martin, P., Tims, S., Mc Gill, A., Ryan, B. and Pfitzner, K., 2006.** Use of airborne gamma-ray spectrometry for environmental assessment of the rehabilitated Nabarlek uranium mine, Northern Australia. *Environmental Monitoring and Assessment*, V. 115, pp. 531–553.
- Nimeck, G. and Koch, R., 2008.** A progressive geophysical exploration strategy at the Shea Creek uranium deposit. *The Leading Edge*, V. 27, No. 1, pp. 52–63.
- Oskooi, B., 2004.** A broad view on the interpretation of electromagnetic data (VLF, RMT, MT, CSTMT). Uppsala University, Sweden.
- Oskooi, B. and Pedersen, L.B., 2001.** Processing and interpretation of tensor VLF data. Report to the Geological Survey of Sweden.
- Plumlee, G., Smith, K.S., Ficklin, W. and Briggs, P. H., 1992.** Geological and geochemical controls on the composition of mine drainages and natural drainages in mineralized areas. Proceedings, 7th International Water-Rock Interaction Conference; Park City, Utah, USA. pp. 419–422.
- Reid, A.B., Allsop, J.M., Granser, H., Millett, A.J. and Somerton, I.W., 1990.** Magnetic interpretation in three dimensions using Euler deconvolution. *Geophysics*, V. 55, pp. 80–90.
- Sharma, S.P. and Baranwal, V.C., 2005.** Delineation of groundwater-bearing fracture zones in a hard rock area integrating very low frequency electromagnetic and resistivity data. *Journal of Applied Geophysics*, V. 57, pp. 155–166.
- Smith, R.S., Annan, A.P., McGowan, P.D., 2001.** A comparison of data from airborne, semi-airborne, and ground electromagnetic systems. *Geophysics* 66, 1379–1385.
- Thompson, D.T., 1982.** EULDPH: A new technique for making computer-assisted depth estimates from magnetic data. *Geophysics*, V. 47, pp. 31–37.
- Tuncer V., Unsworth M.J., Siripunvaraporn W., and Craven J.A., 2006.** Exploration for unconformity-type uranium deposits with audiomagnetotelluric data: a case study from the McArthur River mine, Saskatchewan, Canada, *Geophysics*, V. 71, No. 6, pp. B201–B209.
- Vasanthi, A., Sharma, K.K., and Mallick, K., 2006.** On new standards for reducing gravity data: The North American Gravity Database, *Geophysics*, V. 71, pp. 31–32.
- Winkelmann, I., Thomas, M. and Vogel, K., 2001.** Aerial measurements on uranium ore mining, milling and processing areas in Germany. *Journal of Environmental Radioactivity*, V. 53, pp. 301–311.
- Yamaguchi, S., Murakami, T. and Inokuchi, H., 2001.** Resistivity mapping using the VLF-MT method around surface fault ruptures of the 1995 Hyogo-ken Nanbu earthquake, Japan. *The Island Arc*, V.10, pp. 296–305.